Synchronous Overmodulation Control of Cascaded Inverters for Photovoltaic Application

Valentin OLESCHUK, Roman PRUDEAK, Alexandr SIZOV
Power Engineering Institute of the Academy of Sciences
str. Academiei nr. 5, Chisinau, MD-2028, Republic of Moldova
oleschukv@hotmail.com

***Abstract* — Novel method of synchronized pulsewidth modulation (PWM) has been disseminated for control of cascaded (dual) inverters of photovoltaic installation with relatively low DC-voltages of two insulated photovoltaic panels. Control regimes are characterized by overmodulation control modes of two inverters in this case. Algorithms of synchronized PWM provide continuous voltage synchronization both in each inverter and in the load in the overmodulation control zone of inverters. Special attention has been given to analysis of operation of photovoltaic systems with different DC-voltages of two strings of photovoltaic panels. Results of simulations present a behavior of dual-inverter photovoltaic system with two discontinuous and one combined versions of synchronized PWM.**

***Index Terms* — Photovoltaic power systems, Pulse width modulated power converters, Synchronization, Voltage control.**

I. NOMENCLATURE

F – Fundamental frequency
F_s – Switching frequency
i – Number of notches inside a half of the clock-interval
K_s – Coefficient of synchronization
K_{ov1} – The first coefficient of overmodulation
K_{ov2} – The second coefficient of overmodulation
m_H, m_L – Modulation indices of two inverters
THD – Total Harmonic Distortion factor of the phase voltage
V_H, V_L – DC-links voltages
V_{1H}, V_{2H}, V_{3H} – Pole voltages of the first inverter
V_{1L}, V_{2L}, V_{3L} – Pole voltages of the second inverter
V_{1H2H}, V_{1L2L} – Line voltages of two inverters
V_0 – Zero sequence voltage
V_1, V_2, V_3 – Phase voltages of the system
V_{1k} – Amplitude of the k-harmonic of the phase voltage
β_1 - Duration of the central active switching signal inside the clock-interval
β_j - Duration of other active switching signals
γ_j - Duration of the minor part of the active switching signals
λ_j - Duration of notches
τ - Duration of sub-cycles (switching interval)

II. INTRODUCTION

Multilevel converters and drives are a subject of increasing interest in the last years due to some advantages compared with conventional three-phase systems.

Some of the perspective topologies of power converters are now cascaded (dual) two-level converters which utilize two standard three-phase voltage source inverters [1]-[3]. In particular, dual-inverter-based open-end winding motor drives have some advantages such as redundancy of the space-vector combinations and the absence of neutral point fluctuations [4]-[7]. These new drive topologies provide also one of the best possible use of semiconductor switches.

Almost all versions of classical space-vector PWM are based on an asynchronous principle, which results in sub-harmonics (of the fundamental frequency) in the spectrum of the output voltage and current of converters, which are very undesirable for high power applications [8],[9].

In order to provide voltage synchronization in dual-inverter fed drives, a novel method of synchronized PWM has been applied for control of these systems with single DC voltage source [10], and for the systems with two DC sources: without power balancing between sources [11], and also with power balancing PWM algorithms in a linear control range [12].

Besides adjustable speed AC drives, photovoltaic systems are among perspective areas of application of the dual-inverter topology [13],[14]. In particular, Fig. 1 presents dual inverter system supplied by two insulated strings of photovoltaic panels with the resulting DC voltages V_L and V_H [13].

Direct connection of photovoltaic modules to inverters, or their connection through DC/DC link (dashed lines in Fig. 1) is available in this case. Dual inverters are connected to a grid by a three-phase transformer with the open winding configuration on primary side, and this configuration is one of the most suitable for photovoltaic systems with a higher power range.

So, this paper presents analysis of operation of dual-inverter-based photovoltaic system with synchronized PWM with relatively low DC-link voltages of two strings of photovoltaic panels. Control regimes are characterized by overmodulation control modes of two inverters in this case.

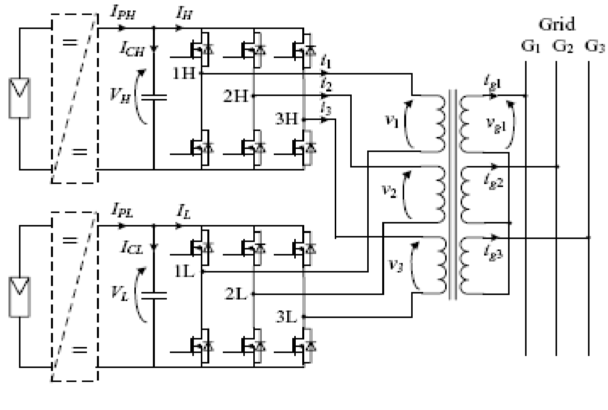

Fig. 1. Topology of dual-inverter-based photovoltaic system [13].

III. BASIC PROPERTIES OF THE METHOD OF SYNCHRONIZED PULSEWIDTH MODULATION

In order to avoid asynchronism of conventional space-vector modulation, novel space-vector-based method of synchronized PWM [15] can be used for control of each inverter in a dual-inverter system for photovoltaic generation.

Figs. 2 - 3 present switching state sequences of standard three-phase inverter inside the interval 0^0-90^0. It illustrates schematically two basic discontinuous versions of space-vector PWM (Fig. 2: DPWM30 – the scheme with the 30^0-non-switching intervals; Fig. 3: DPWM60– scheme with the 60^0-non-switching intervals), which are the most suitable for control of inverters in the zone of overmodulation [8],[15].

The upper traces in Figs. 2 – 3 are switching state sequences (in accordance with conventional designation [15]), then – the corresponding pole voltages of standard three-phase inverter. The lower traces in Figs. 2 - 3 show the corresponding quarter-wave of the line-to-line output voltage of the inverter. Signals βj represent total switch-on durations during switching cycles τ, signals γ_k are generated in the centers of the corresponding β. Widths of notches λ_k represent duration of zero states [15].

So, one of the basic ideas of the proposed PWM method is in continuous synchronization of the positions of all central β_1-signals in the centers of the 60^0-clock-intervals (to fix positions of the β_1-signals in the centers), and then – to generate symmetrically all other active β - and γ-signals, together with the corresponding notches.

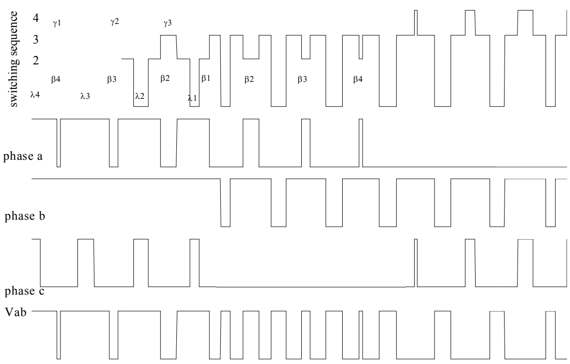

Fig. 2. Switching state sequence, pole voltages V_a, V_b, V_c, and line-to-line voltage V_{ab} of standard three-phase inverter with discontinuous PWM with the 30^0-non-switching intervals (DPWM30).

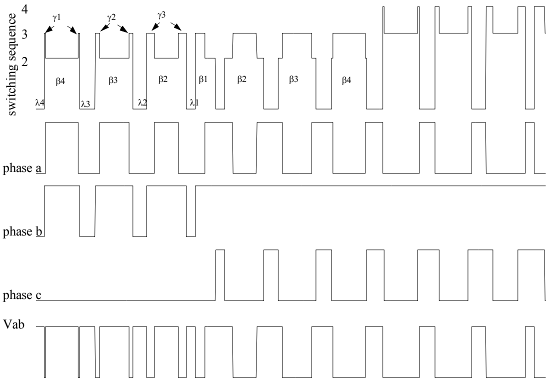

Fig. 3. Switching state sequence, pole voltages V_a, V_b, V_c, and line-to-line voltage V_{ab} of standard three-phase inverter with discontinuous PWM with the 60^0-non-switching intervals (DPWM60).

For the presented photovoltaic power conversion system (Fig. 1) rational determination of the switching frequency Fs of inverters and duration of sub-cycles τ, providing continuous voltage synchronization during fluctuation of the grid fundamental frequency F, can be based on (1),(2) for discontinuous versions of modulation (DPWM) [14]:

$$F_{s(DPWM)} = F(8n-5) \tag{1}$$

$$\tau_{DPWM} = 1/[6F(2n-1.5)], \tag{2}$$

where $n=2,3,4\ldots$.

A set of control correlations for determination of duration of active control signals and notches of invertors with synchronized PWM includes six basic functions [15]. At the same time, in order to provide synchronous and symmetrical control of the output voltage of inverters during overmodulation (modulation index of each inverter is $m>0.907$ in this case), special coefficients of overmodulation K_{ov1} and K_{ov2} have to be used for correction of duration of active control signals of dual-inverter system during specific two-stage control algorithm in the zone of overmodulation [16]. The fist stage of overmodulation control zone is observed, if modulation indices of inverters are equal to $0.952>m>0.907$; and at the second stage of overmodulation zone modulation indices of inverters are equal to: $1>m>0.952$.

In particular, during the fist stage of overmodulation control of dual-inverter-based photovoltaic system, the first coefficient of overmodulation K_{ov1} has to be used for correction of duration of the β-signals (see Figs. 2-3). In this case, if $m<0.907$, $K_{ov1}=1$, and if $0.952>m>0.907$:

$$Kov1=1-(m-0.907)/0.045 \tag{3}$$

Also, the second coefficient of overmodulation K_{ov2} has to be used for correction of duration of the γ-signals (see Figs. 2-3) in the second part of the overmodulation control zone. In particular, if $m<0.952$, $K_{ov2}=1$, and if $1>m>0.952$:

$$K_{ov2}=1-(m-0.952)/0.048 \tag{4}$$

So, the described algorithm provides smooth symmetrical pulses ratio changing of the output voltage of dual-inverter system during the whole overmodulation control zone.

IV. SYNCHRONOUS OPERATION OF DUAL INVERTERS IN THE OVERMODULATION ZONE

Synchronous control of the output voltage of each inverter of dual-inverter-based system with algorithms of synchronized PWM provides synchronous symmetrical regulation of the phase voltages V_1, V_2 and V_3 of the system. Rational phase shift between waveforms of the output voltages of the two inverters is equal in this case to one half of the switching interval (sub-cycle) τ [1].

In the case, when the two DC-link voltage sources have equal voltages ($V_H=V_L$), the resulting voltage space-vectors are equal to the space-vector patterns of conventional three-level inverter [1],[3],[6].

The phase voltages V_1, V_2, V_3 of the dual-inverter system with two isolated DC-sources (Fig. 1) are calculated in accordance with (5)-(8) [4]:

$$V_0 = 1/3(V_{1L} + V_{2L} + V_{3L} + V_{1H} + V_{2H} + V_{3H}) \quad (5)$$

$$V_1 = V_{1L} + V_{1H} - V_0 \quad (6)$$

$$V_2 = V_{2L} + V_{2H} - V_0 \quad (7)$$

$$V_3 = V_{3L} + V_{3H} - V_0, \quad (8)$$

where V_{1L}, V_{2L}, V_{3L}, V_{1H}, V_{2H}, V_{3H} are the corresponding pole voltages of each three-phase inverter (Fig. 1), V_0 is zero sequence (triplen harmonic component) voltage.

Control of photovoltaic power conversion systems on the base of dual inverters has some peculiarities. In particular, in the case of direct connection between the two photovoltaic strings and the two inverters, in order to provide maximum power point tracking of photovoltaic panels, control of the system should be based on the corresponding specific regulation of modulation indices of dual inverters [13]. And this control is somewhat similar to power sharing process between two dual inverters for traction systems, analyzed in [7],[12].

Flexible PWM control of cascaded inverters with space-vector pulsewidth modulation for photovoltaic application, providing stabilization of the magnitude of the fundamental harmonic of the phase voltages, can be performed by the specialized control system [13]. In particular, in the case of higher DC-link voltages (this control mode corresponds to higher level of solar irradiance), modulation indices of the two modulated inverters should be decreased correspondingly, in order to provide nearly constant amplitude of the phase voltage during solar irradiance fluctuations.

In the case of low DC-links voltages (it corresponds to low solar irradiance) modulation indices m_H and m_L of two inverters should be high. And, in particular, in the case of higher modulation indices of dual inverters, when $m>0.907$ (it corresponds to overmodulation control mode), control of the system should be based on special two-stage control scheme with specialized PWM algorithm [8],[15],[16].

A. The First Stage of Overmodulation Control Mode

During the first stage of the overmodulation control mode, when $0.952>m>0.907$, a smooth linear increase of the β-parameters until the width of $\beta_1 = \tau$ is observed for each inverter of the dual-inverter system, with simultaneous smooth reduction of duration of all notches λ [16].

As an example of operation of the dual-inverter system with synchronized PWM with relatively low DC voltages, when $m=m_H=m_L=0.95$ (control regime corresponds to the first stage of overmodulation mode in this case), Fig. 4 – Fig. 9 present basic voltage waveforms (period of the pole voltages V_{1H}, V_{1L},, line-to-line voltages V_{1H2H}, V_{1L2L} of the two inverters, and of the phase voltage V_1 (with its spectrum in Figs. 5, 7, 9) of the system. Fundamental frequency of the system is $F=50Hz$, and average switching frequency is $F_s = 1.35\ kHz$ for each modulated inverter.

Figs. 4 - 5 show basic voltage waveforms (with spectrum of the phase voltage V_1) of the system with discontinuous synchronized PWM with the 30^0-non-switching intervals (DPWM30, see Fig. 2). Figs. 6-7 present the corresponding voltage waveforms (with spectrum of the V_1 voltage) of the system with discontinuous synchronized PWM with the 60^0-non-switching intervals (DPWM60, Fig. 3), and Figs. 8-9 illustrate behavior of the system with combined DPWM30+ DPWM60 control of dual inverters.

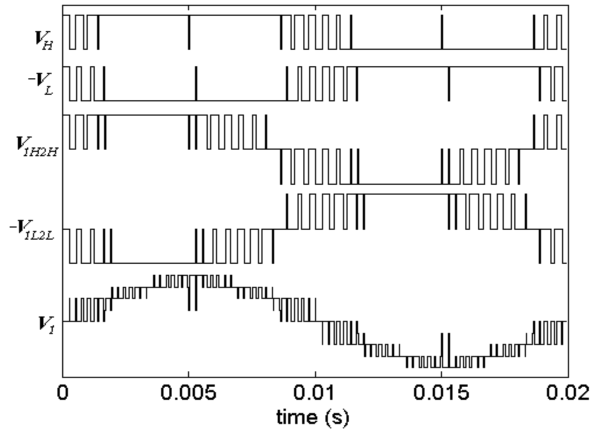

Fig. 4. Pole voltages V_{1H} and V_{1L}, line voltages V_{1H2H} and V_{1L2L}, and phase voltage V_1 of the system with discontinuous synchronized PWM in the first part of overmodulation zone (DPWM30, $F=50Hz$, $m=m_H=m_L=0.95$).

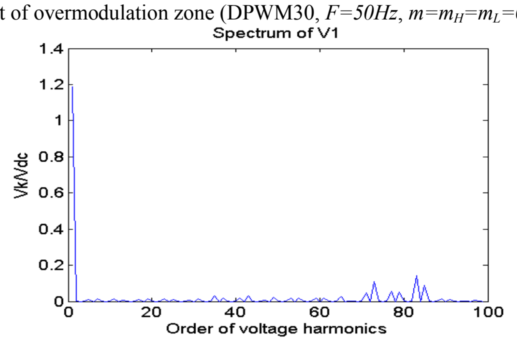

Fig. 5. Spectrum of the V_1 voltage of the system with discontinuous PWM (DPWM30, $F=50Hz$, $F_s=1.35kHz$, $V_{dc}=V_H=V_L$, $m=m_H=m_L=0.95$).

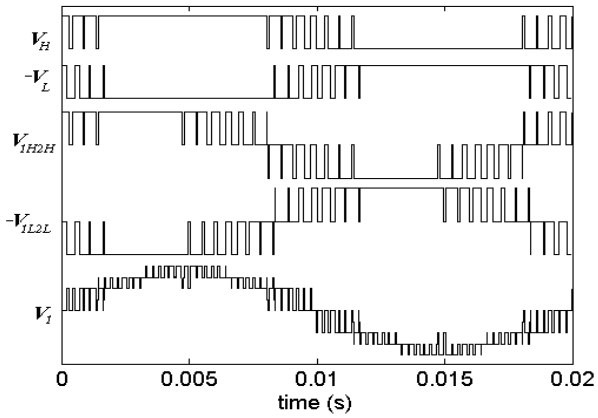

Fig. 6. Pole voltages V_{1H} and V_{1L}, line voltages V_{1H2H} and V_{1L2L}, and phase voltage V_1 of the system with discontinuous synchronized PWM in the first part of overmodulation zone (DPWM60, $F=50Hz$, $m=m_H=m_L=0.95$).

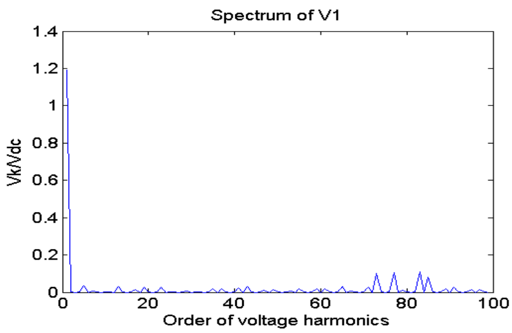

Fig. 7. Spectrum of the V_1 voltage of the system with discontinuous PWM (DPWM60, $F=50Hz$, $F_s=1.35kHz$, $V_{dc}=V_H=V_L$, $m=m_H=m_L=0.95$).

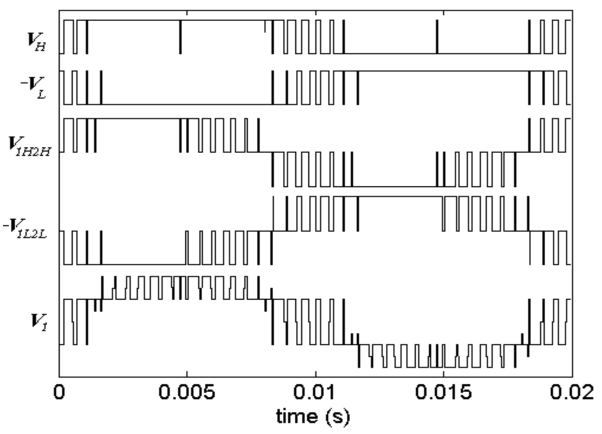

Fig. 8. Pole voltages V_{1H} and V_{1L}, line voltages V_{1H2H} and V_{1L2L}, and phase voltage V_1 of the system with combined synchronized PWM (DPWM30+ DPWM60, $F=50Hz$, $F_s=1.35kHz$, $V_{dc}=V_H=V_L$, $m=m_H=m_L=0.95$).

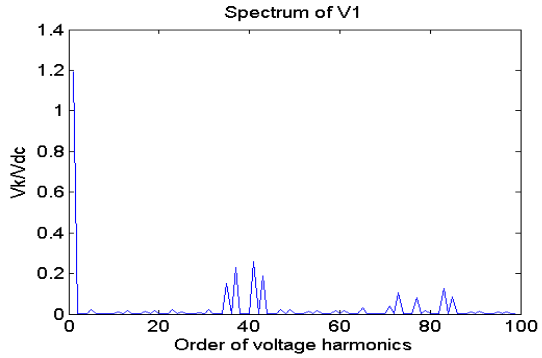

Fig. 9. Spectrum of the V_1 voltage of the system with combined synchronized PWM (DPWM30+DPWM60, $F=50Hz$, $V_{dc}=V_H=V_L$, $m=m_H=m_L=0.95$).

B. The Second Stage of Overmodulation Control Mode

The second sub-zone of the system control during overmodulation, when $1>m>0.952$, is characterized by a smooth decrease until close to zero value of durations of all γ -signals of dual inverters [15],[16].

As an example of operation of the dual-inverter system with synchronized PWM with the lowest DC-voltages (it correspond to control in the second part of overmodulation zone, when $m=m_H=m_L=0.99$), Fig. 10 – Fig. 15 present basic voltage waveforms of the dual-inverter system (with spectrum of the phase voltage in Figs. 11, 13, 15). Figs. 10-11 correspond to the system with synchronized DPWM30 control; Figs. 12-13 correspond to dual-inverter system with synchronized DPWM60 control, and Figs. 14-15 illustrate behavior of the system with combined DPWM30+DPWM60 control of dual inverters. Fundamental frequency of the system is $F=50Hz$, and average switching frequency is $F_s=1.35kHz$ for each modulated inverter.

In the case of the minimum (threshold) level of solar irradiance (and the minimum magnitude of the DC-voltage of photovoltaic panels ($V_{dc}=V_H=V_L=V_{dc-min}$)) modulation indices of dual inverters of photovoltaic system should have the maximum value $m=m_H=m_L=1$. So, this control mode corresponds to a six-step operation of each inverter of the system, and Fig. 16 illustrates this control regime.

Analysis of spectral characteristics of the phase voltage of the dual-inverter system operating in the zone of overmodulation (see Figs. 5, 7, 9, 11, 13, 15) shows, that due to the algorithms of synchronized PWM the spectra of the phase voltage do not contain even harmonics and sub-harmonics for any operation conditions of photovoltaic system.

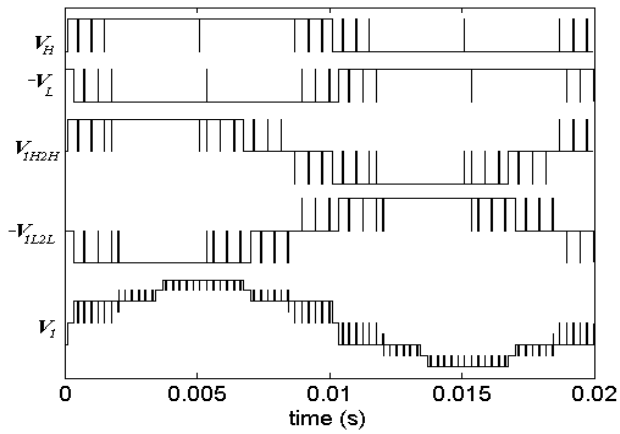

Fig. 10. Pole voltages V_{1H} and V_{1L}, line voltages V_{1H2H} and V_{1L2L}, and phase voltage V_1 of the system with discontinuous synchronized PWM in the second part of overmodulation zone (DPWM30, $F=50Hz$, $m=m_H=m_L=0.99$).

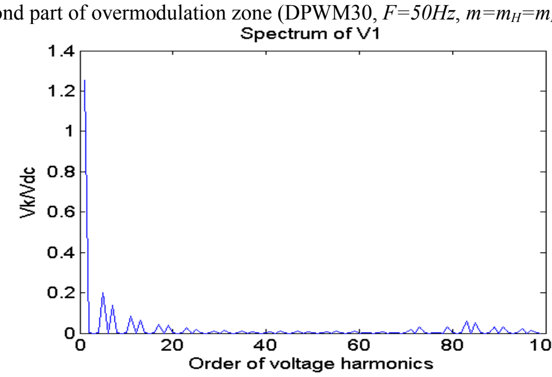

Fig. 11. Spectrum of the V_1 voltage of the system with discontinuous PWM (DPWM30, $F=50Hz$, $F_s=1.35kHz$, $V_{dc}=V_H=V_L$, $m=m_H=m_L=0.99$).

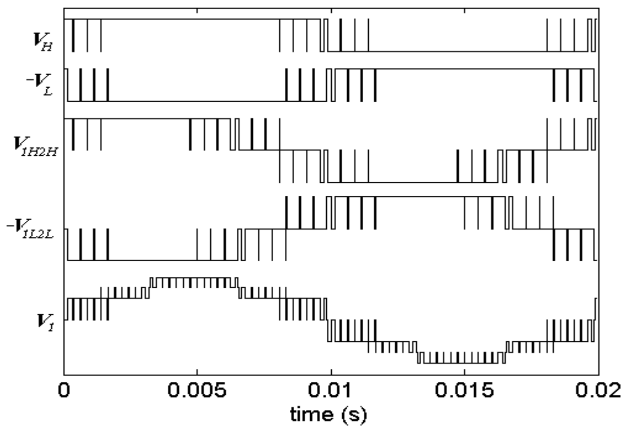

Fig. 12. Pole voltages V_{1H} and V_{1L}, line voltages V_{1H2H} and V_{1L2L}, and phase voltage V_1 of the system with discontinuous synchronized PWM in the second part of overmodulation zone (DPWM60, $F=50Hz$, $m=m_H=m_L=0.99$).

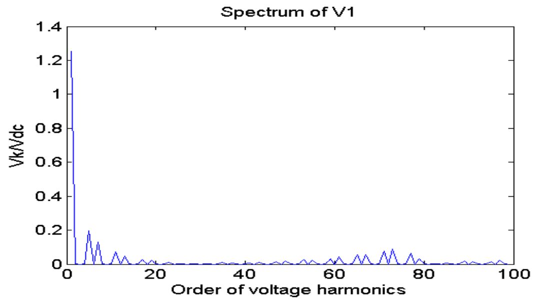

Fig. 13. Spectrum of the V_1 voltage of the system with discontinuous PWM (DPWM60, $F=50Hz$, $F_s=1.35kHz$, $V_{dc}=V_H=V_L$, $m=m_H=m_L=0.99$).

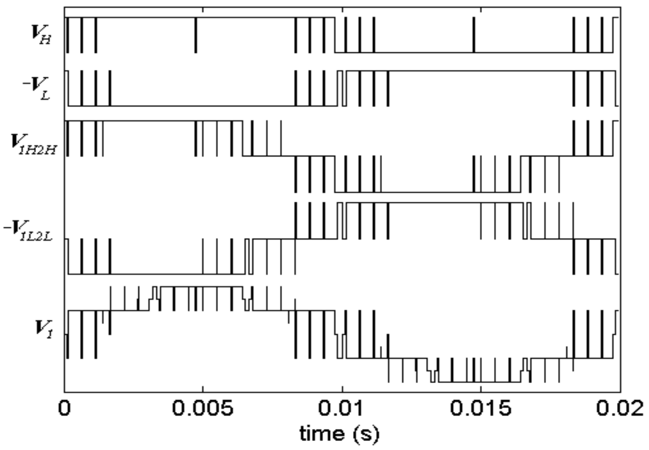

Fig. 14. Pole voltages V_{1H} and V_{1L}, line voltages V_{1H2H} and V_{1L2L}, and phase voltage V_1 of the system with combined synchronized PWM (DPWM30+ DPWM60, $F=50Hz$, $F_s=1.35kHz$, $V_{dc}=V_H=V_L$, $m=m_H=m_L=0.99$).

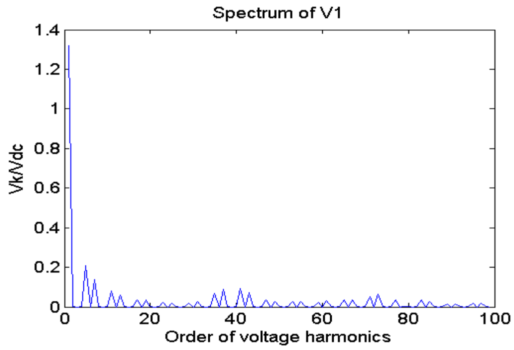

Fig. 15. Spectrum of the V_1 voltage of the system with combined synchronized PWM (DPWM30+DPWM60, $F=50Hz$, $V_{dc}=V_H=V_L$, $m=m_H=m_L=0.99$).

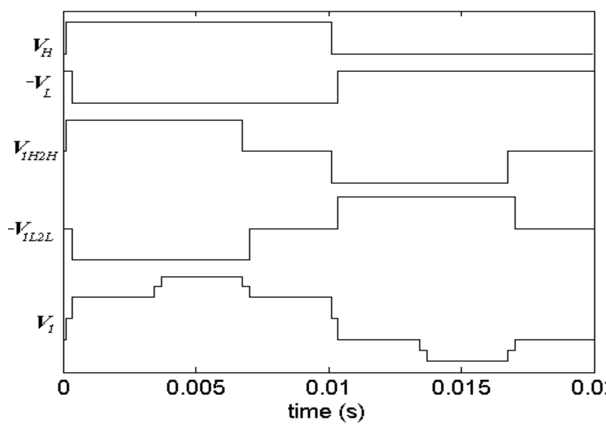

Fig. 16. Basic voltage waveforms of the system with maximum modulation indices of dual inverters ($F=50Hz$, $V_{dc}=V_{dc\text{-}min}=V_H=V_L$, $m=m_H=m_L=1$).

C. Overmodulation PWM Control of Dual-Inverter System with Non-Equal DC-Voltages

In the case of different level of solar irradiance for the two strings of photovoltaic panels, the corresponding DC-voltages V_H and V_L in the system (see Fig. 1) are different too. In order to provide maximum power point tracking of photovoltaic panels and stabilization of the magnitude of the fundamental harmonic of the phase voltage of a dual-inverter photovoltaic system, modulation indices m_H and m_L of the two inverters should be in inversely proportional quantities with the corresponding DC-voltages [13],[14].

Fig. 17 illustrates operation of photovoltaic system under condition $V_H=0.75V_L$ (modulation indices of the two inverters are mH=0.99 and mL=0.75 in this case). Fig. 18 presents spectrum of the phase voltage of the system. In particular, harmonic analysis of voltage waveforms shows that spectra of the phase voltage of dual-inverter systems with synchronized pulsewidth modulation do not contain even harmonics and sub-harmonics in systems with both equal and different voltages of two DC-sources.

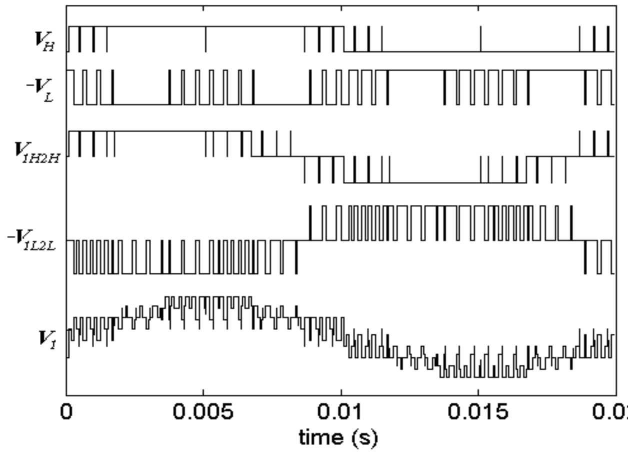

Fig. 17. Pole voltages V_{1H} and V_{1L}, line voltages V_{1H2H} and V_{1L2L}, and phase voltage V_1 of the system with discontinuous synchronized PWM with different DC-voltages (DPWM30, $F=50Hz$, $V_H/V_L=0.75$, $m_H=0.99$, $m_L=0.75$).

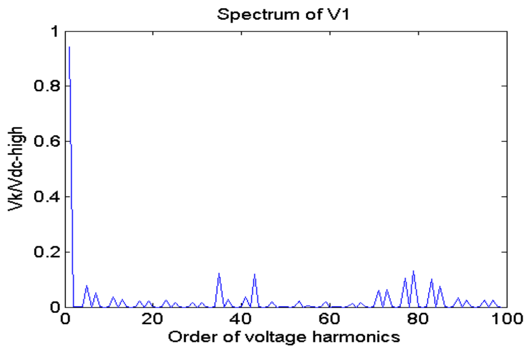

Fig. 18. Spectrum of the V_1 voltage of the system with discontinuous synchronized PWM (DPWM30, $F=50Hz$, $V_H/V_L=0.75$, $m_H=0.99$, $m_L=0.75$).

V. SPECTRAL ASSESSMENT OF PHASE VOLTAGE QUALITY OF DUAL-INVERTER SYSTEM

Total Harmonic Distortion (*THD*) factor of voltage and current is one of the most suitable criteria for analysis of power quality in grid-connected photovoltaic systems. In particular, in accordance with the majority of standards for 50-Hz power systems, total voltage harmonic distortion has to be calculated up to the 40th voltage harmonic [17].

Fig. 19 presents the calculation results of Total Harmonic Distortion factor (*THD*) for the phase voltage V_1 as a function of modulation index $m=m_H=m_L$, of the dual-inverter-based system with equal DC-link voltages ($V_{dc}=V_H=V_L$), controlled by algorithms of two discontinuous (DPWM30 and DPWM60) and one combined (DPWM30+DPWM60) schemes of synchronized modulation. The *THD* factor ($THD=(1/V_{1_1})\sqrt{\sum_{k=2}^{40} V_{1_k}^2}$) has been calculated until the 40-th low-order (*k*-th) voltage harmonic. The fundamental frequency of the system is *50Hz*, and the average switching frequency of each modulated inverter is equal to *1.35 kHz*.

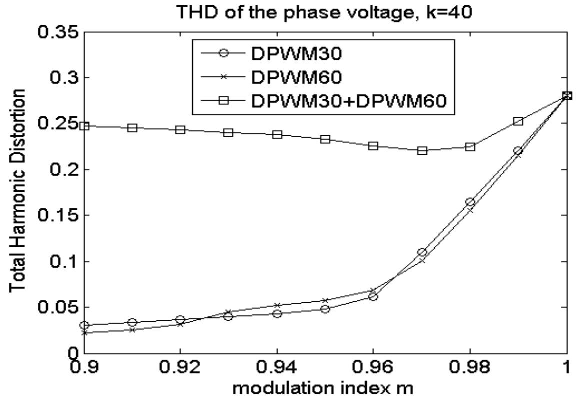

Fig. 19. *THD* factor of the phase voltage V_1 versus modulation index $m= m_H=m_L$ for the systems with two discontinuous (DPWM30 and DPWM60) and combined (DPWM30+DPWM60) versions of synchronized PWM (*k=40*).

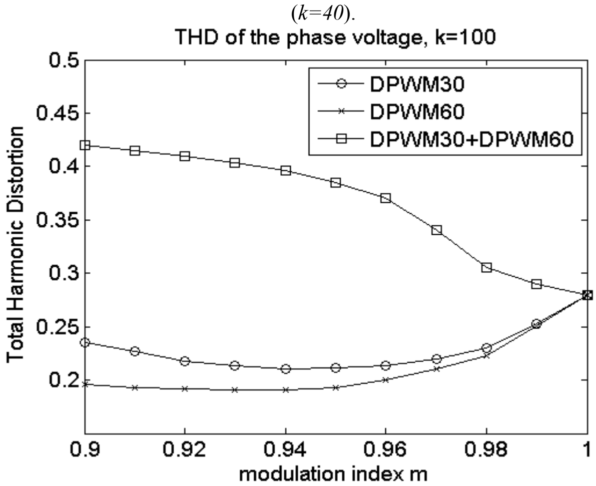

Fig. 20. *THD* factor of the phase voltage V_1 versus modulation index $m= m_H=m_L$ for the systems with two discontinuous (DPWM30 and DPWM60) and combined (DPWM30+DPWM60) versions of synchronized PWM (*k=100*).

It is interesting also to calculate *THD* factor for increased number of low order voltage harmonics of the phase voltage. In particular, Fig. 20 shows the calculation results for the case, when *THD* factor of the phase voltage of the system has been calculated until the 100-th low-order (*k*-th) voltage harmonic.

The presented calculation results show, that values of Total Harmonic Distortion factor of the phase voltage of dual-inverter system are close for the systems controlled by the both basic versions of discontinuous synchronized pulsewidth modulation (DPWM30 or DPWM60), but combined version of modulation (DPWM30+DPWM60) does not provide good quality of spectral composition of the phase voltage in the overmodulation control zone of inverters.

VI. CONCLUSION

Novel method of synchronized pulsewidth modulation has been disseminated for control of cascaded (dual) inverters of photovoltaic installation operating with relatively low DC-voltages of two insulated photovoltaic panels. Control regimes are characterized by overmodulation control modes of two inverters in this case. The proposed determination of switching frequencies of the two inverters in accordance with (1)-(2) allows continuous phase voltage synchronization during fluctuation of the grid fundamental frequency. And correction of duration of all control signals by the means of special coefficients of overmodulation (3)-(4) provides smooth symmetrical pulses ratio changing of the output voltage of the system during overmodulation control zone.

The spectra of the phase voltages of synchronized dual-inverter installations do not contain in this case even harmonics and sub-harmonics for any operating conditions of the systems with both equal and different voltages of the two DC-sources (photovoltaic panels). It has been shown also, that two alternative schemes of discontinuous synchronized PWM provide almost equivalent level of phase voltage distortion during overmodulation control of dual inverters.

REFERENCES

[1] H. Stemmler and P. Guggenbach, “Configurations of high power voltage source inverter drives”, Proc. of the EPE’93 Conf., pp. 7-12.
[2] H. Stemmler, “High-power industrial drives”, IEEE Proc., vol. 82, no. 8, pp. 1266-1286, 1994.
[3] K.A. Corzine, S.D. Sudhoff and C.A. Whitcomb, “Performance characteristics of a cascaded two-level converter”, IEEE Trans. Energy Conversion, vol. 14, no. 6, pp. 433-439, 1999.
[4] E.G. Shivakumar, K. Gopakumar, S.K. Sinha, A. Pittet and V.T. Ranganathan, “Space vector PWM control of dual inverter fed open-end winding induction motor drive”, Proc. of the IEEE APEC’2001 Conf., pp. 399-405.
[5] E.G. Shivakumar, V.T. Somasekhar, K.K. Mohapatra, K. Gopakumar, L. Umanand and S.K. Sinha, “A multi level space phasor based PWM strategy for an open-end winding induction motor drive using two inverters with different dc-link voltages”, Proc. of the IEEE PEDS’2001 Conf., pp. 169-175.
[6] M.R. Baiju, K.A. Mohapatra, R.S. Kanchan and K. Gopakumar, “A dual two-level inverter scheme with common mode voltage elimination for an induction motor drive”, IEEE Trans. Power Electr., vol. 19, no. 6, pp. 794-805, 2004.
[7] G. Grandi, C. Rossi, A. Lega and D. Casadei, “Multilevel operation of a dual two-level inverter with power balancing capability”, CD-ROM Proc. of the IEEE IAS’2006 Conf., 8 p.
[8] J. Holtz, “Pulsewidth modulation – a survey”, IEEE Trans. Ind. Electr., vol. 39, no. 5, pp. 410-420, 1992.
[9] N. Mohan, T.M. Undeland and W.P. Robbins, Power Electronics, 3rd ed. John Wiley & Sons, 2003.
[10] V. Oleschuk, F. Profumo, G. Griva, R. Bojoi and A.M. Stankovic, “Analysis and comparison of basic schemes of synchronized PWM for dual inverter-fed drives”, Proc. of the IEEE ISIE’2006 Symp., pp. 2455-2461.
[11] V. Oleschuk, A. Sizov, F. Profumo, A. Tenconi and A.M. Stankovic, “Multilevel dual inverter-fed drives with synchronized PWM”, CD-ROM Proc. of the IEEE PESC’2006 Conf., 7 p.
[12] V. Oleschuk, R. Bojoi, G. Griva and F. Profumo, “Dual inverter-fed traction drives with DC sources power balancing based on synchronized PWM”, Proc. of the IEEE IEMDC’2007 Conf., pp. 260-265.
[13] G. Grandi, D. Ostojic, C. Rossi and A. Lega, “Control strategy for a multilevel inverter in grid-connected photovoltaic applications”, CD-ROM Proc. of the IEEE 2007 Aegean Conf. on Electr. Machines, Power Electr. and Electromotion, 6 p.
[14] G. Griva and V. Oleschuk, “Dual inverters with synchronized PWM for grid-connected photovoltaic systems”, Proc. of the IEEE ICCEP’2009 Conf., pp. 420-425.
[15] V. Oleschuk and F. Blaabjerg, “Direct synchronized PWM techniques with linear control functions for adjustable speed drives”, Proc. of the IEEE APEC’2002 Conf., pp. 76-82.
[16] V. Oleschuk, V. Ermuratski and E.M. Chekhet, “Drive converters with synchronized pulsewidth modulation during overmodulation,” Proc. of the IEEE ISIE’2004 Symp., pp. 1339-1344
[17] M. Aiello, A. Cataliotti, S. Favuzza and G. Graditi, “Theoretical and experimental comparison of Total Harmonic Distortion factors for the evaluation of harmonic and interharmonic pollution of grid-connected photovoltaic systems”, IEEE Trans. Power Delivery, vol. 21, no. 3, pp. 1390-1397, 2006.